21. Fogarty, P., Kalpin, R. F. & Sullivan, W. The *Drosophila* maternal-effect mutation *grapes* causes a metaphase arrest at nuclear cycle 13. *Development* **120,** 2131–2142 (1994).
22. Francesconi, S., Grenon, M., Bouvier, D. & Baldacci, G. p56^{chk1} protein kinase is required for the DNA replication checkpoint at 37 °C in fission yeast. *EMBO J.* **16,** 1332–1341 (1997).
23. Walworth, N. C. & Bernards, R. rad-dependent response of the chk1-encoded protein kinase at the DNA damage checkpoint. *Science* **271,** 353–356 (1996).
24. Raff, J. W. & Glover, D. M. Nuclear and cytoplasmic cycles continue in *Drosophila* embryos in which DNA synthesis is inhibited with aphidicolin. *J. Cell Biol.* **107,** 2009–2019 (1988).
25. Banga, S. S., Shenkar, R. & Boyd, J. B. Hypersensitivity of *Drosophila mei-41* mutants to hydroxyurea is associated with reduced mitotic chromosome stabiity. *Mutant. Res.* **163,** 157–165 (1986).
26. Shermoen, A. W. & O'Farrell, P. H. Progression of the cell cycle through mitosis leads to abortion of nascent transcripts. *Cell* **67,** 303–310 (1991).
27. Ruden, D. M. & Jackle, H. Mitotic delay dependent survival identifies components of cell cycle control in the *Drosophila* blastoderm. *Development* **121,** 63–73 (1995).
28. Theurkauf, W. E. in *Methods of Cell Biology:* Drosophila melanogaster*: Practical Uses in Cell and Molecular Biology* (eds Goldstein, L. S. B. & Fryberg, E.) 489–505 (Academic, New York, 1994).
29. Tautz, D., Pfeifle, C. A non-radioactive in situ hybridization method for the localization of specific RNA's in *Drosophila* embryo's reveals translational control of the segmentation gene *hunchback*. *Chromosoma* **98,** 81–85 (1989).

Acknowledgements. We thank W. Sullivan, S. Campbell, B. Holdener, J. Kramer, N. Hollingsworth and B. Eggen for comments on the manuscript; B. Edgar and P. O'Farrell for discussions; P. Gergen for probes and advice on whole-mount *in situ* hybridization; P. Fogarty and W. Sullivan for sharing unpublished data and providing *grp* cDNA clones; R. S. Hawley and colleagues at the University of California at Davis for providing their collection of P-element-associated maternal-effect lethal mutations; and B. Edgar for anti-Cdc2 antibodies and advice on cell-cycle control during early embryogenesis. This work was supported by a fellowship from the NWO to O.C.M.S. and grants from the NIH and American Cancer Society to W.E.T.

Correspondence and requests for materials should be addressed to W.E.T. (e-mail: theurk@mcbsgi.bio.sunysb.edu).

Structure of the multimodular endonuclease *Fok*I bound to DNA

David A. Wah, Joel A. Hirsch*, Lydia F. Dorner†, Ira Schildkraut† & Aneel K. Aggarwal*

Department of Biochemistry and Molecular Biophysics, Columbia University, New York, New York 10032, USA
† New England Biolabs, 32 Tozer Road, Beverly, Massachusetts 01915, USA

***Fok*I is a member of an unusual class of bipartite restriction enzymes that recognize a specific DNA sequence and cleave DNA nonspecifically a short distance away from that sequence[1–3]. Because of its unusual bipartite nature, *Fok*I has been used to create artificial enzymes with new specificities[4–7]. We have determined the crystal structure at 2.8 Å resolution of the complete *Fok*I enzyme bound to DNA. As anticipated, the enzyme contains amino- and carboxy-terminal domains corresponding to the DNA-recognition and cleavage functions, respectively. The recognition domain is made of three smaller subdomains (D1, D2 and D3) which are evolutionarily related to the helix–turn–helix-containing DNA-binding domain of the catabolite gene activator protein CAP[8]. The CAP core has been extensively embellished in the first two subdomains, whereas in the third subdomain it has been co-opted for protein–protein interactions. Surprisingly, the cleavage domain contains only a single catalytic centre, raising the question of how monomeric *Fok*I manages to cleave both DNA strands. Unexpectedly, the cleavage domain is sequestered in a 'piggyback' fashion by the recognition domain. The structure suggests a new mechanism for nuclease activation and provides a framework for the design of chimaeric enzymes with altered specificities.**

*Fok*I exists as a monomer and recognizes an asymmetric DNA sequence 5′-GGATG-3′, cleaving DNA phosphodiester groups 9 and 13 base pairs (bp) away from the recognition site (Fig. 1). The structure shows the enzyme approaching DNA from the major-groove side, where it appears to surround the DNA (Fig. 2). Subdomain D1 of the recognition domain covers the DNA major groove, recognizing base pairs at the 3′ end of the recognition sequence (GGATG). D1 is a compact structure of eight helices (α1 to α8), two loops (L1 and L2), a β-sheet (β1 to β3) and an N-terminal arm (Fig. 3a). Helices α4, α5 and α6 and loops L1 and L2 make up the modified helix–turn–helix (HTH) motif. The short helices α4 and α5 share the same helical axis, as if they were part of a single α-helix into which L1 has been inserted. Together, α4 and α5 (α4/5) form the first helix of the HTH motif; α6 is the second helix (also known as the recognition helix) which lies against the DNA major groove. The turn expected between α4/5 and α6 is replaced by L2. Both loops reach out like fingers from the helices to make base-specific contacts with the DNA. D1 connects to D2, which contacts base pairs at the 5′ end of the recognition sequence (GGATG). D2 is an extended, triangular-shaped structure of six helices (α1 to α6), a β-sheet (β1, β2, β5), a β-hairpin (β3, β4), and a short loop L1 (Fig. 3a). As in D1, the basic HTH motif is extensively modified. α2 and α5 comprise the two α-helices of the HTH motif, with α5 lying in the DNA major groove. The 'turn' is replaced by loop L1, a pair of antiparallel helices α3 and α4, and a short segment T1 connecting α4 to α5. D3 is most similar to CAP and related proteins such as histone H5, HNF-3γ and the biotin operon repressor (BirA)[8–11] (Fig. 3a). Despite this similarity, D3 barely touches the DNA. Remarkably, its recognition helix lies outside the DNA major groove and is used primarily to piggyback the cleavage domain onto the recognition domain. Thus, we observe an almost identical HTH motif being used in a different context. In the CAP-related protein–DNA complexes, the motif is used to recognize the DNA bases, whereas in D3 the motif is used primarily to mediate protein–protein interactions.

As already noted, subdomains D1 and D2 make almost all of the base-specific contacts with the DNA. The DNA maintains a B-form DNA conformation without any major bends or kinks. Interactions between D1 and DNA occur along four segments of the subdomain. The N-terminal arm, loop L1, and the recognition helix α6 form specific contacts in the major groove, whereas loop L2 makes contacts in the minor groove. D2, on the other hand, contacts DNA exclusively in the major groove by α4 and T1 of the 'turn', and the recognition helix α5. The recognition helices of D1 and D2 approach DNA differently. The D1 recognition helix is most similar to the canonical form, packing against the major groove with its α-helical axis roughly perpendicular to the DNA axis[12]. In contrast, the recognition helix of D2 juts away from the DNA, its α-helical axis tilted by ~35° with respect to the plane of the base pairs. The 'angle of attack' is reminiscent of the way the α-helices of the zinc-fingers of protein Zif268 approach DNA[13]. As a unit, the HTH of D2 is flipped 180° with respect to the HTH of D1, analogous to the inverse orientations of the HTH motifs of the homeodomain and the POU-specific domain of the Oct-1 POU domain[14].

The protein–DNA interactions are extensive. For instance, almost all of the hydrogen-bond donor and acceptor groups in the major groove of the recognition sequence are involved in direct contacts with the protein. This complementarity at the protein–DNA interface ensures that only the *Fok*I recognition sequence can form all of the interactions. The three guanines of the recognition sequence (GGATG) make bidentate hydrogen bonds with arginine and lysine residues, and the adenines of the third and fourth base

Figure 1 Sequence of the 20-bp DNA fragment used to co-crystallize *Fok*I. The recognition sequence is numbered and the sites of cleavage are indicated by arrows. Asterisks denote the thymine residues substituted by iodouracils in the derivative Iodo (Table 1). This oligomer can be cleaved by the enzyme (data not shown).

* Present addresses: Department of Molecular Biophysics and Biochemistry, Yale University, New Haven, Connecticut 06511, USA (J.A.H.); Department of Physiology and Biophysics, Mount Sinai School of Medicine, New York, New York 10029, USA (A.K.A.).

pairs (GGATG) form bidentate hydrogen bonds with glutamine and asparagine residues (see Fig. 3b,c for details). We also observe novel interactions involving an aromatic tryptophan residue (Trp 105), which is wedged against the non-polar edges of three consecutive pyrimidines of base pairs 4 to 6 (GGATGA) in the major groove with impressive van der Waals complementarity (Fig. 3c). To our knowledge, this is the first time that a tryptophan residue has been observed in such a context, and it appears to represent a particularly efficient way of specifying consecutive pyrimidine residues in the major groove.

The cleavage domain has a structure remarkably similar to a subunit of the dimeric endonuclease *Bam*HI (ref. 15) (Fig. 4). The resemblance was unexpected as the two enzymes lack sequence similarity. Furthermore, *Bam*HI exists as a dimer and cleaves at a specific DNA site, and *Fok*I exists as a monomer and cleaves at a nonspecific site[15]. The *Fok*I cleavage domain has a compact α/β architecture consisting of a mixed six-stranded β-sheet (β1 to β6) with α-helices (α1, α2, α3, α6 and α4, α5) on each side (Fig. 4). The similarity with *Bam*HI allows us to align the active sites of the two enzymes, which occur at the end of a β-meander formed by strands β1, β2, β3 in *Fok*I and strands β3, β4, β5 in *Bam*HI (Fig. 4). Remarkably, the three residues Asp 450, Asp 467 and Lys 469 that are important for catalysis in *Fok*I (ref. 16) overlap exactly with the catalytic residues Asp 94, Glu 111 and Glu 113 of *Bam*HI (ref. 15). The identification of only a single catalytic centre raises the question of how monomeric *Fok*I manages to cleave both DNA strands. Consistent with the notion of a single active site, it has been shown that changing either Asp 450 or Asp 467 to an alanine in *FokI* results in the loss of cleavage of both DNA strands[16]. Thus, in order for the enzyme to cleave both strands, we suggest that it either dimerizes on DNA or that its cleavage domain flips between two orientations, cleaving first one DNA strand and then the other.

Probably the most surprising feature of our complex is the position of the cleavage domain (Fig. 2). Our expectation was that the cleavage domain would be located in a major groove, cleaving DNA one turn away from the recognition sequence.

Table 1 Crystallographic analysis

	Native	Hg 1*	Hg 2*	Hg 3*	Au	Sm	Iodo
Detector	CCD	CCD	IPs	CCD	CCD	CCD	IPs
Resolution (Å)	2.8	3.0	3.0	3.0	3.0	4.1	3.0
Unique reflections	26,243	17,014	18,759	20,950	16,268	7,046	20,397
Data coverage (%)	98.5	78	87	97	75	82	94
R_{merge} (%)†	7.5	6.2	8.0	7.5	4.6	2.8	8.2
Phasing statistics:							
R_{iso} (%)‡		9.0	8.1	10.2	7.1	7.7	14.4
Phasing power (isomorphous)§		1.74	1.73	1.41	1.35	1.45	
Phasing power (anomalous)‖			1.38	1.35	1.85	1.68	
Refinement statistics: (8 to 2.8 Å)							
Reflections, $F > 2\sigma(F)$	24,931						
R-factor (%)	21.4						
R-free (%)¶	29.6						
R.m.s. bond lengths (Å)	0.011						
R.m.s. bond angles (°)	1.7						

CCD, charge-coupled device; IPs, imaging plates.
* The mercurial derivatives differ in the times of soak and the relative occupancies and positions of the heavy-atom sites.
† $R_{merge} = \Sigma |I_{obs} - \langle I \rangle| / \Sigma \langle I \rangle$, calculated for all data.
‡ $R_{iso} = \Sigma |F_p - F_{ph}| / \Sigma F_p$, where F_p and F_{ph} are the structure factor amplitudes of the native and derivative data, respectively.
§ Phasing power (isomorphous) = $\langle |F_h| \rangle$/r.m.s.(ϵ), where $\langle |F_h| \rangle$ is the mean calculated amplitude for the heavy-atom model and ϵ is the lack of closure error.
‖ Phasing power (anomalous) = $\langle |\Delta F_h| \rangle$/r.m.s.($\epsilon'$), where $\langle |\Delta F_h| \rangle$ is the mean calculated Bijvoet difference from the heavy-atom model and ϵ' is the lack of closure for anomalous differences.
¶ Calculated with 3% of the reflection data excluded from refinement.

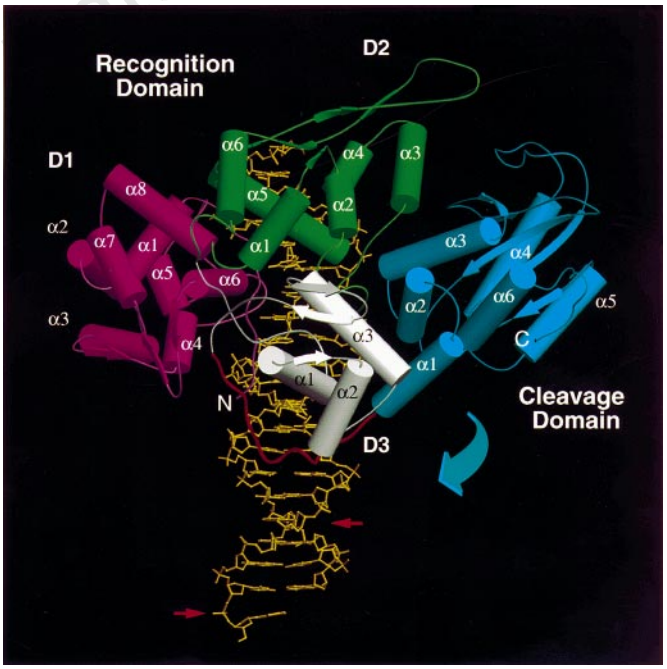

Figure 2 The complete *Fok*I enzyme (579 amino acids) bound to DNA. The recognition domain consists of three smaller subdomains D1, D2 and D3 shown in purple, green and white, respectively. The cleavage domain is shown in blue and the linker segment connecting it to the recognition domain is shown in red. The DNA (yellow) is the 20-bp DNA fragment shown in Fig. 1. Small arrows indicate the sites of cleavage. The large arrow conveys the proposed motion of the cleavage domain toward the cleavage site. The structure assignment is as follows: D1, α1(17–25), α2(32–45), α3(49–58), β1(66–67), α4(68–72), L1(73–86), α5(87–91), L2(92–103), α6(104–116), β2(120–123), β3(128–131), α7(133–140), α8(146–156); D2, α1(160–168), β1(175–176), α2(177–182), L1(183–196), α3(197–205), α4(211–218), T1(219–221), α5(222–236), β2(240–242), β3(245–248), β4(258–261), β5(264–267), α6(269–277); D3, α1(303–319), β1(323–324), α2(325–335), α3(341–353), β2(358–361), β3(364–367); linker (373–387); cleavage domain, α1(389–400), α2(406–414), α3(421–434), β1(439–442), β2(451–454), β3(462–469), α4(479–491), β4(514–521), α5(528–539), β5(543–547), α6(548–560), β6 (575–576).

Instead, we find that the cleavage domain is packed alongside the recognition domain and is prevented from associating with the DNA-cleavage site. This is in agreement with footprinting studies on *Fok*I with DNA which show a lack of protection at the cleavage site[16–18]. From our structure, the cleavage domain can be brought to the major groove for cleavage by simple rotations around the linker segment. The sequestering of the cleavage domain may explain how *Fok*I manages to regulate its cleavage activity until it is required. The compact configuration we observe may be the state in which the enzyme scans the DNA looking for the correct site, and upon finding it, in the presence of Mg^{2+}, the cleavage domain swings over to the major groove for DNA cleavage. The recognition domain sequesters the cleavage domain through an extensive set of protein–protein interactions (Fig. 5). These interactions are primarily electrostatic and mediated by subdomains D2 and D3 of the recognition domain, the linker segment, and helices α1 and α3 and strand β1 of the cleavage domain.

For the enzyme to become activated for cleavage, these protein–protein interactions would need to be replaced by intermolecular interactions with the DNA. The binding of Mg^{2+} may provide part of the free energy for the configurational switch of the enzyme by promoting the formation of the active site. Evidence for sequestration of the cleavage domain by the recognition domain also comes from an unusual class of mutants[19], isolated using a genetic screen to identify amino-acid substitutions that enable *Fok*I to cleave DNA in cells expressing the cognate methylase activity. When applied to the restriction endonuclease *Eco*RI, a similar screen produced mutants that cleaved DNA at non-cognate sites and the mutations occurred in residues involved in DNA recognition[20]. In the *Fok*I screen, eight mutations (G188K, P196S, T343I, S388N, S395F, E407K, E410K, D421N) were reported and two (P196S, D421N) were studied in detail[19]. Unlike *Eco*RI, both of these mutants cleaved only at the cognate *Fok*I site, including hemimethylated sites in which one or the other DNA strand was methylated. Remarkably, we find that seven of the eight mutations occur at the interdomain interface and would be expected to relax the domain–domain association (Fig. 5). The mutants T343I, S388N and S395F would disrupt the hydrogen-bonding network between residues Ser 395, Lys 387 and Glu 339 that connects the cleavage domain to D3. Mutants G188K, E407K and E410K insert a positive charge in the vicinity of residue Lys 427, destabilizing the electrostatic environment at the interface. Replacement of Pro 196 with a serine residue will weaken a key hydrophobic interaction between D2 and helix α3 of the cleavage domain, and may also disrupt a nearby hydrogen bond between Ser 194 and Lys 427. To explain their data, Waugh and Sauer postulated that there may be a rate-limiting step in the *Fok*I cleavage reaction that involves the dissociation of the cleavage domain from the recognition domain which is accelerated by these mutants to allow cleavages of even hemimethylated DNA sites[19]. The compact nature of our complex and the mapping of these mutations to the interdomain interface is consistent with this new mechanism of enzyme activation.

The *Fok*I complex has implications for the evolution of HTH proteins. The *Fok*I structure reveals unprecedented modifications to the basic CAP core, including the insertion of large loops and secondary structural elements in subdomains D1 and D2. These extra elements act as additional prongs both to grip the DNA and to mediate protein–protein interactions between the subdomains. These embellishments are so extensive that the structural alignment program DALI (ref. 21) was needed to elucidate the CAP core. The D3 recognition helix lies outside the major groove, suggesting that the HTH motif can perform other roles besides DNA recognition. An analogous mechanism can be found in multi-zinc-finger proteins such as TFIIIA[22,23] and GLI[24], in which some zinc-fingers penetrate the DNA major groove to recognize specific base pairs, and others lie outside the major groove to fulfil other functions. The evolutionary success of the HTH motif in both prokaryotes and eukaryotes appears to be due partly to its versatility in accommodating modifications both in structure and in function.

Finally, the *Fok*I complex provides a framework for the design of

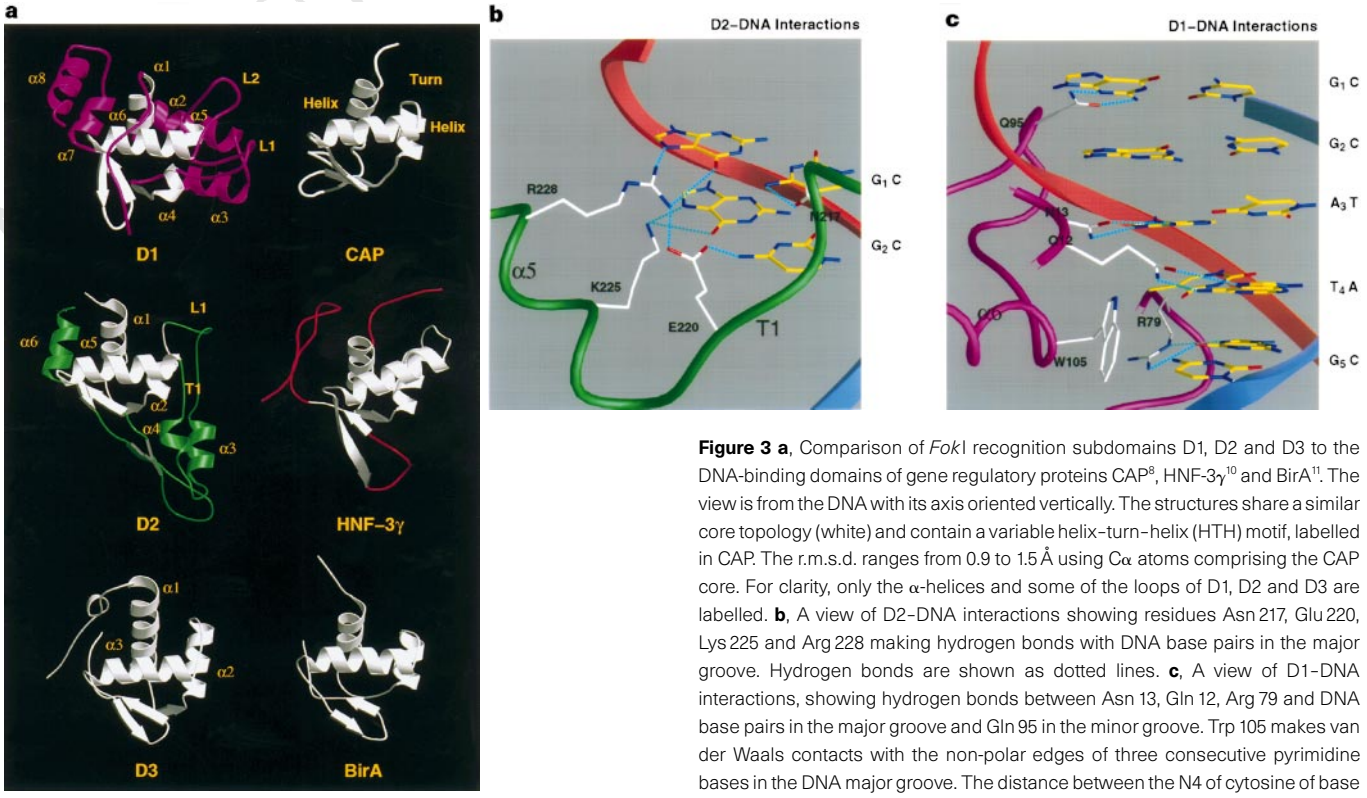

Figure 3 a, Comparison of *Fok*I recognition subdomains D1, D2 and D3 to the DNA-binding domains of gene regulatory proteins CAP[8], HNF-3γ[10] and BirA[11]. The view is from the DNA with its axis oriented vertically. The structures share a similar core topology (white) and contain a variable helix–turn–helix (HTH) motif, labelled in CAP. The r.m.s.d. ranges from 0.9 to 1.5 Å using Cα atoms comprising the CAP core. For clarity, only the α-helices and some of the loops of D1, D2 and D3 are labelled. **b**, A view of D2–DNA interactions showing residues Asn 217, Glu 220, Lys 225 and Arg 228 making hydrogen bonds with DNA base pairs in the major groove. Hydrogen bonds are shown as dotted lines. **c**, A view of D1–DNA interactions, showing hydrogen bonds between Asn 13, Gln 12, Arg 79 and DNA base pairs in the major groove and Gln 95 in the minor groove. Trp 105 makes van der Waals contacts with the non-polar edges of three consecutive pyrimidine bases in the DNA major groove. The distance between the N4 of cytosine of base pair G_5C and the tryptophan indole ring is 3.9 Å, ruling out a strong aromatic hydrogen bond.

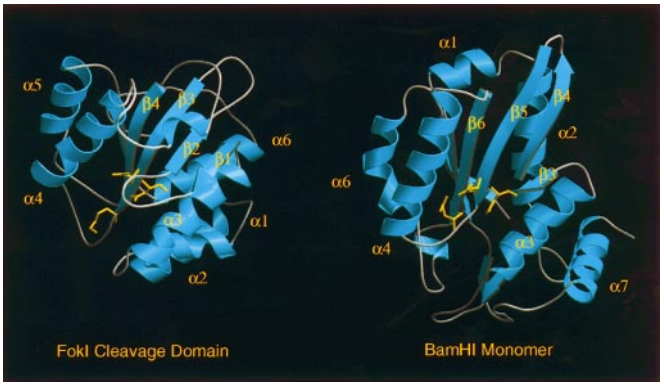

Figure 4 Comparison of *Fok*I cleavage domain to a monomer of endonuclease *Bam*HI. The two structures share a similar β-sheet core surrounded by α-helices on both sides, and superimpose with an r.m.s.d. of 2.0 Å using 61 Cα atoms. The active-site residues of both nucleases occur at one end of the β-sheet and are shown in yellow.

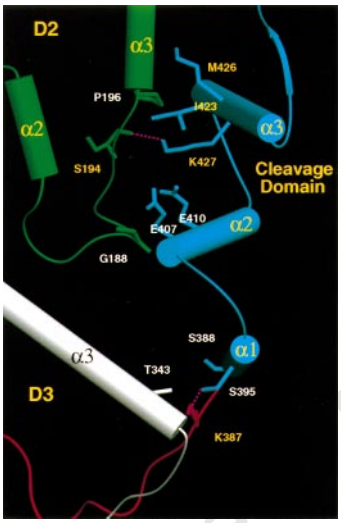

Figure 5 The new class of *Fok*I mutants (labelled in white) identified by Waugh and Sauer[19] map to the interdomain interface between the recognition domain and the cleavage domain. The mutations appear to disrupt the interdomain interface, allowing the cleavage domain more readily to dissociate from the recognition domain and swing over to the DNA major groove for cleavage.

new restriction enzymes. Chimaeric enzymes can be created by attaching the cleavage domain of *Fok*I to the DNA-binding domains of transcription factors. The structure allows a definition of the linker segment precisely (residues 373 to 387) and allows a modelling of the *Fok*I cleavage domain alongside the DNA-binding domains of various transcription factors. The zinc-finger transcription factors Zif268 and Sp1 have received particular attention owing to the possibility of selecting and swapping fingers to create new specificities[5,6]. The mechanism of nuclease activation implied by our structure may be an additional feature that could be incorporated into the design of artificial enzymes as a way of regulating their activity. □

Methods

*Fok*I was expressed, purified and co-crystallized with a 20-bp DNA oligonucleotide in 2.2 M ammonium sulphate[25]. The co-crystals diffract to 2.8 Å when cooled to −160 °C and exposed to synchrotron radiation. They belong to space group $P2_1$ with unit cell dimensions of $a = 65.6$ Å, $b = 119.3$ Å, $c = 71.5$ Å, and $\beta = 101.4°$, and contain a single protein–DNA complex per asymmetric unit. Data were measured at the Cornell High Energy Synchrotron Source (CHESS), using both the charge-coupled device (CCD) detector (beamline A1) and imaging plates (beamline F1) at $\lambda = 0.908$ Å (Table 1). Most of the heavy-atom derivatives were prepared by conventional soaks in different heavy-atom solutions. The Iodo derivative was prepared by substituting iodouracils for four thymine residues on the DNA fragment (Fig. 1). The heavy-atom positions were refined with PHASIT[26] and the resulting MIRAS (multiple isomorphous replacement including anomalous scattering) phases were used to calculate a 3.5 Å map that was continuous and showed clear electron density for the DNA. The position of the DNA matched the iodouracil positions determined from the Iodo derivative. The MIRAS map was further improved by cycles of solvent flattening with SOLOMON[27]. Using these and subsequent partial model phase combined maps, interspersed with positional and simulated annealing refinements using X-PLOR[28], we built 562 residues of the protein and the complete DNA molecule with program O[29]. Residues 1–3, 252–254 and 282–286 could not be built owing to uninterpretable density. The positional and temperature factor refinements were extended to 2.8 Å resolution[28], and the model was verified through extensive simulated annealing omit maps. Near the end of refinement, 172 water molecules were added to the model (B-values <65 Å^2) from the inspection of $F_o - F_c$ maps.

Received 23 December 1996; accepted 23 April 1997.

1. Sugisaki, H. & Kanazawa, S. New restriction endonucleases from *Flavobacterium okeanokoites* (*Fok*I) and *Micrococcus luteus* (*Mlu*I). *Gene* **16,** 73–78 (1981).
2. Li, L., Wu, L. P. & Chandrasegaran, S. Functional domains of *Fok*I restriction endonuclease. *Proc. Natl Acad. Sci. USA* **89,** 4275–4279 (1992).
3. Skowron, P., Kaczorowski, T., Tucholski, J. & Podhajska, A. J. Atypical DNA-binding properties of class-IIS restriction endonucleases: evidence for recognition of the cognate sequence by a *Fok*I monomer. *Gene* **125,** 1–10 (1993).
4. Kim, Y.-G. & Chandrasegaran, S. Chimeric restriction endonuclease. *Proc. Natl Acad. Sci. USA* **91,** 883–887 (1994).
5. Kim, Y.-G., Cha, J. & Chandrasegaran, S. Hybrid restriction enzymes: Zinc finger fusions to *Fok*I cleavage domain. *Proc. Natl Acad. Sci. USA* **93,** 1156–1160 (1996).
6. Huang, B., Schaeffer, C. J., Li, Q. & Tsai, M.-D. Splase: a new class IIs zinc-finger restriction endonuclease with specificity for SP1 binding sites. *J. Prot. Chem.* **15,** 481–489 (1996).
7. Podhajska, A. J. & Szybalski, W. Conversion of the *Fok*I endonuclease to a universal restriction enzyme: cleavage of phase M13mp7 DNA at predetermined sites. *Gene* **40,** 175–182 (1985).
8. Schultz, S. C., Shields, G. C. & Steitz, T. A. Crystal structure of a CAP–DNA complex: the DNA is bent by 90 degrees. *Science* **253,** 1001–1007 (1991).
9. Ramakrishnan, V., Finch, J. T., Graziano, V., Lee, P. L. & Sweet, R. M. Crystal structure of globular domain histone H5 and its implications for nucleosome binding. *Nature* **362,** 219–223 (1993).
10. Clark, K. L., Halay, E. D., Lai, E. & Burley, S. K. Co-crystal structure of the HNF-3γ DNA recognition motif resembles histone H5. *Nature* **364,** 412–420 (1993).
11. Wilson, K. S., Shewchuk, L. M., Brennan, R. G., Otsuka, A. J. & Matthews, B. W. *Escherichia coli* biotin holoenzyme synthetase/biorepressor crystal structure delineates biotin- and DNA-binding domains. *Proc. Natl Acad. Sci USA* **89,** 9257–9261 (1992).
12. Harrison, S. C. & Aggarwal, A. K. DNA recognition by proteins with the helix-turn-helix motif. *Annu. Rev. Biochem.* **59,** 933–969 (1990).
13. Pavletich, N. P. & Pabo, C. O. Zinc finger–DNA recognition: crystal structure of a zif268–DNA complex at 2.1 Å resolution. *Science* **252,** 809–817 (1991).
14. Klemm, J. D., Rould, M. A., Aurora, R., Herr, W. & Pabo, C. O. Crystal structure of Oct-1 POU domain bound to an octamer site: DNA recognition with tethered DNA-binding modules. *Cell* **77,** 21–32 (1994).
15. Newman, M., Strzelecka, T., Dorner, L. F., Schildkraut, I. & Aggarwal, A. K. Structure of restriction endonuclease *Bam*HI and its relationship to *Eco*RI. *Nature* **268,** 660–664 (1994).
16. Waugh, D. S. & Sauer, R. T. Single amino acid substitutions uncouple the DNA binding and strand scission activities of *Fok*I endonuclease. *Proc. Natl Acad. Sci. USA* **90,** 9596–9600 (1993).
17. Yonezawa, A. & Sugiura, Y. DNA binding mode of class-IIS restriction endonuclease *Fok*I revealed by DNA footprinting analysis. *Biochem. Biophys. Acta* **1219,** 369–379 (1994).
18. Li, L., Wu, L. P., Clarke, R. & Chandrasegaran, S. C-terminal deletion mutants of the *Fok*I restriction endonuclease. *Gene* **133,** 79–84 (1993).
19. Waugh, D. S. & Sauer, R. T. A novel class of *Fok*I restriction endonuclease mutants that cleave hemimethylated substrates. *J. Biol. Chem.* **269,** 12298–12303 (1994).
20. Heitman, J. & Model, P. Mutants of the *Eco*RI endonuclease with promiscuous substrate specificity implicate residues involved in substrate recognition. *EMBO J.* **9,** 3369–3378 (1990).
21. Holm, L. & Sander, C. J. Protein structural comparison by alignment of distance matrices. *J. Mol. Biol.* **233,** 123–138 (1993).
22. Churchill, M. E., Tullius, T. D. & Klug, A. Mode of interaction of the zinc finger protein TFIIIA with a 5S RNA gene of *Xenopus*. *Proc. Natl Acad. Sci. USA* **87,** 5528–5532 (1990).
23. Clemens, K. R., Liao, X., Wolf, V., Wright, P. E. & Gottesfeld, J. M. Definition of the binding sites of individual zinc fingers in the transcription factor IIIA-5S RNA gene complex. *Proc. Natl Acad. Sci. USA* **89,** 10822–10826 (1992).
24. Pavletich, N. P. & Pabo, C. O. Crystal structure of a five-finger GL1-DNA complex: new perspectives on Zn fingers. *Science* **261,** 1701–1707 (1993).
25. Hirsch, J. A., Wah, D. A., Dorner, L. F., Schildkraut, I. & Aggarwal, A. K. Crystallization and preliminary X-ray analysis of restriction endonuclease *Fok*I bound to DNA. *FEBS Lett.* **403,** 136–138 (1997).
26. Furey, W. *Phases—A Program Package for the Processing and Analysis of Diffraction Data for Macromolecules* (VA Medical Center, Pittsburgh, PA, 1993).
27. Abrahams, J. P. & Leslie, A. G. W. Methods used in the structure determination of bovine mitochondrial F_1 ATPase. *Acta Crystallogr. D* **52,** 30–42 (1996).
28. Brunger, A. T. *X-PLOR, Version 3.1, A System for X-ray Crystallography and NMR* (Yale University, New Haven, CT, 1992).
29. Jones, T. A., Zou, J.-Y. & Cowan, S. W. Improved methods for building models in electron density maps and the location of errors in these models. *Acta Crystallogr. A* **47,** 110–119 (1991).

Acknowledgements. We thank the staff at CHESS and C. Escalante, E. Jacobson, M. Newman and H. Viadiu for help with data collection; R. Knott for DNA synthesis; and T. Bestor, W. Hendrickson, R. Mann and R. Roberts for comments on the manuscript. This work was supported by an NIH grant (A.K.A.) and NIH training grants (J.A.H. and D.A.W.).

Correspondence and requests for materials should be addressed to A.K.A. (e-mail: aggarwal@inka.mssm.edu). Coordinates have been deposited in the Brookhaven Protein Data Bank under accession number 1FOK.